Control of deeply-buried Proterozoic basement intrusive rocks inferred from a basin-wide maps of interval-specific geothermal gradient, Delaware Basin, West Texas, and southeastern New Mexico

Chesney Petkovsek, Paul Mann, and Andrew Pepper, Department of Earth and Atmospheric Sciences, University of Houston*

Summary

Previously proposed ideas for explaining the geothermal gradient of the Delaware Basin of west Texas and New Mexico include: 1) localized heating from Eocene-Miocene intrusive rocks within the western sedimentary fill of the basin (Manos and Perez, 2018); 2) heating from radiogenic decay of minerals within Proterozoic sialic intrusive rocks within the crystalline basement that underlies the sedimentary basin (Pepper et al., 2020); 3) Intra-basinal circulation of hot fluids along fault zones; 4) deep burial by late Cretaceous Laramide foreland basin clastic rocks eroded from the Laramide orogeny to the west of the basin; 5) combined effects of the above sources. Each of the five proposed sources of heat flow are associated with tectonic events which have reactivated faults and produced igneous intrusive rocks. In this study we have used gravity, magnetic, 3D seismic grids, and wells to basement to demonstrate how Precambrian basement features control temperature gradients, gas-to-oil ratios of Wolfcampian source rocks, and controlled sweet spots for both conventional and unconventional production. We present preliminary findings of this ongoing study.

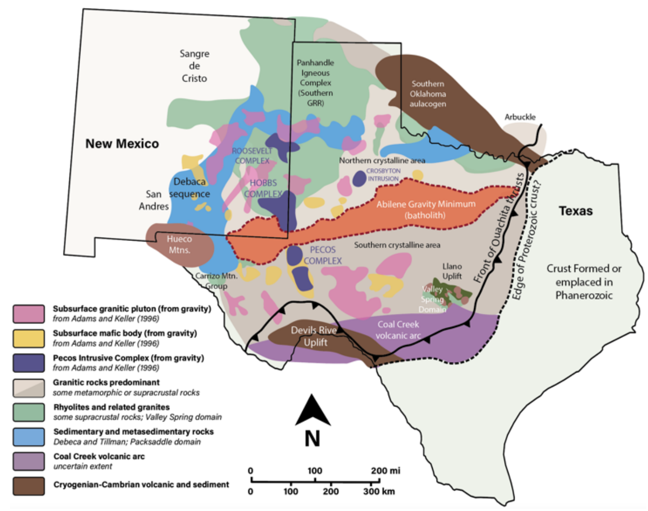

Figure 1: Proterozoic basement lithologies and major tectonic elements compiled from Adams and Keller (1996); Mosher (1998); Barnes et al. Ewing et al., (2019), Adams and Keller (1996), and Ewing et al. (2019).

Introduction and tectonic setting

With 15 billion barrels of total oil and gas equivalent production, the West Texas Permian Basin is recognized as a hydrocarbon super basin according to Whaley (2019), Fryklund and Stark (2020) and Sternbach (2020). The basin is a complexly structured intracratonic foreland basin overlying a Proterozoic basement that has been subject to multiple stages of deformation and high rates of subsidence. Increased conventional and unconventional drilling activity throughout the basin reveals highly variable gas-oil ratios produced from Wolfcampian source rocks of the Delaware sub-basin which do not simply follow trends in burial depth (Pepper et al., 2020). The discordance between maturation and burial depth emphasizes the need to explore the influence of various tectonic processes on its thermal and burial history. This study demonstrates the importance of Proterozoic basement features on measured bottom-hole temperatures and corrected geothermal gradient in the Delaware Basin.

The Permian Basin is underlain by highly variable Proterozoic basement that records the deformation and accretion of an outer tectonic belt and the later development of the southern granite-rhyolite province (Adams and Keller, 1996). A prominent geophysical feature related to these early events is the Abilene Gravity Minimum (AGM). Core data from wells drilled to basement within the Abilene Gravity Minimum have penetrated igneous (granitic or granodioritic) and metasedimentary basement types (Adams and Keller, 1996; Ewing et al., 2019). An alternate interpretation of the AGM is that it is a highly, elongated granitic batholith related to the Grenville Orogeny and dated as 1078 ± 23 Ma from a core sample (Ewing et al., 2019). The Central Basin Uplift is underlain by two Middle-Proterozoic mafic intrusions. Pre-Grenville mafic intrusions interpreted from gravity data are distributed throughout the greater Permian Basin (Barnes et. al, 2002). Formation of the southern granite-rhyolite province was followed by a period of rifting or back-arc spreading and of passive continental margin development (Adams and Keller, 1996), followed by a period of deformation and uplift related to the Grenville Orogeny (Adams and Keller, 1996) which led to the initial development of the Permian Basin and termination of the precursory Tobosa Basin in the late Mississippian. The Permian Basin then experienced a main deformational phase characterized by rapid post-Atokan uplift of the Central Basin Platform and subsidence of the Permian Basin

(Gardiner, 1990; Hoak et al, 1998) that led to the formation of the Delaware and Midland sub-basins. During the late Cretaceous to Eocene, the Permian Basin underwent deposition in a foreland basin stretching from Canada to Mexico, followed by rebound and erosion continuing to the present day (Pepper et al., 2020). Following Laramide shortening, intrusive rocks of the middle Eocene to Oligocene Trans-Pecos Igneous Province were distributed over the western Delaware Basin (Brown, 2019).

the true non-linear temperature-depth relationships in basins, however, we use a linear fit here for convenience to illustrate lateral changes. The methodology for basin temperature correction used in this study follows a similar design of a depth varying interval geothermal gradient (IGG) developed by Deighton et al. (2014).

Results

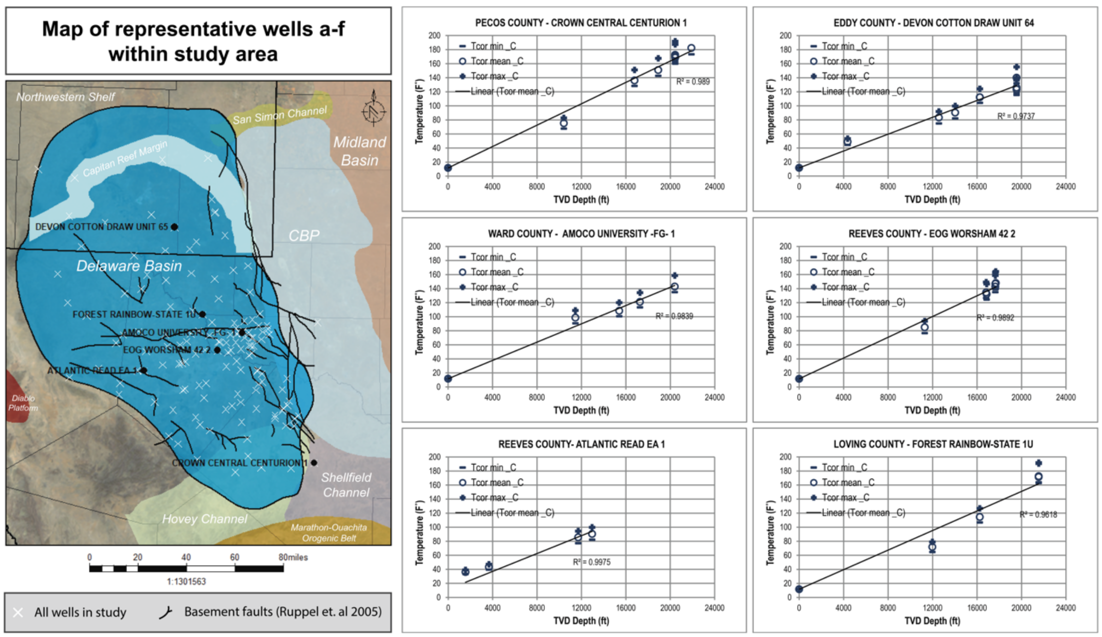

Figure 2: A. Map of six, named wells in the Delaware Basin with the War-Wink single-point correction applied. B. Geothermal gradient values for the six wells with linear best fit lines.

Methods

Raw bottom-hole temperature (BHT) data points were compiled from a dataset of 1,024 well logs that are distributed across the Delaware Basin (Fig. 2). These well logs were based on multiple logging runs within a total of 140 wellbores that penetrated Mississippian-age strata to Proterozoic basement. The well log dataset is a collection of publicly available logs and proprietary raster and digital log files provided by exploration and production operators within the Delaware Basin. Analysis of the 1,024 well logs resulted in 484 raw BHT values and their associated depths of reading that were corrected for drilling and logging parameters that included temperature gauge offset, hole size, drilling fluid, and time since last circulation. We used an annual mean surface temperature of 11.7 °C (53°F) to calculate BHT corrections and corrected gradients. We emphasize that linear geothermal gradients rarely describe

Of the 140 wells included in this study, 23 wells had three or more logging runs at the same TVD depth with unique BHT readings. For these 23 wells, Horner corrections were applied. A single-well temperature correction derived from multiple Horner corrections within a proprietary study in the War-Wink area of eastern Delaware Basin that was previously conducted by A. Pepper. The War-Wink single-point correction was found to calculate BHT values with a <2% error in degrees Celsius and was then applied to all BHT values where the well was unsuitable for a Horner correction. The results of six representative wells after having the War-Wink single point correction applied are shown on Figure 2. These six wells were chosen because of their spatial distribution within the study area, and because these wells penetrate ultra-deep formations that are

Mississippian to Precambrian in age. The data points in these wells are concentrated at similar depths within each well. These depths correspond to common casing points for wells within the Delaware Basin due to changes in geomechanical parameters along the stratigraphic column. The Crown Central Centurion 1 well in Pecos County, Devon Cotton Draw Unit 64 in Eddy County, and the EOG Worsham 42 2 in Reeves County have multiple temperature readings at the same depth and are differentiated only by tool offset. For all six wells, a linear fit from a surface temperature of 53°C does not allow an optimal fit to the BHT associated with the deepest temperature reading. Observed temperature readings at intermediate depths of 9,000-16,000 TVD are overestimated by a linear fit in 5 of the 6 representative wells and underestimated in 1 of the 6 representative wells. The overestimation of temperature at intermediate depths is frequently observed throughout the larger dataset.

We have employed a depth-varying geothermal gradient using a similar process to that developed by Deighton et. al. (2014). Formation tops were picked in all 140 wells from log start to stop. Each observed BHT value was then assigned to a formation based on the formation top picks. The dataset was then divided into four stratigraphic packages for geothermal gradient mapping. The four stratal packages include: 1) Surface to base of Salado (Present – Ochoan); 2) Base of Salado to base of Bone Springs (Ochoan – Leonardian); 3) Base of Bone Spring to base of Wolfcamp (Leonardian – Wolfcampian); 4) Base of Wolfcamp to Precambrian basement (Wolfcampian – Precambrian). Finally, geothermal gradient maps of the four stratal packages were constructed and are shown in Figure 3.

This dataset was focused on wells which penetrate the ultra-deep formations (>17000 ft TVD) within the Delaware Basin that have associated BHT readings. Distribution and density of these temperature points are well distributed throughout the basin. Areas of the most well-related data points correspond to previously active conventional gas fields that targeted structural traps in pre-Pennsylvanian reservoirs and were since converted to injection wells. Data points in the north of the basin are sparse due to the lack of deep reservoir targets related to pre-Pennsylvanian structural traps.

Corrected geothermal gradients in the ultra-deep section (Base of Wolfcamp to Precambrian basement) are shown in Figure 3a and locally correlate with major basin faults and flexures as mapped by Horne et al. (2021 Geothermal gradient values overlying mafic intrusive bodies are generally lower than the ambient geothermal gradient values overlying rhyolitic and/or granitic domains. For example, geothermal gradient values south of the AGM - which do not overlie mafic or granitic intrusive features - fall within the underlying Southern Crystalline Area and are generally higher than those overlying mafic bodies. Overall geothermal gradient values are lowest above the mafic intrusives underlying the Central Basin Platform along the eastern margin of the Delaware Basin. The geothermal gradient increases towards the western edge of the basin and onto the Diablo Platform. Stratal package 4 (Fig. 3a), stratal package 2 (Fig. 3c), and stratal package 1 (Figure 3d) all reflect this westward increase in geothermal gradient. Stratal package 3 (Figure 3b) also shows this westward increase in gradient, with the exception of two cooler data points on the western edge of the basin near the Diablo Platform. The area of high geothermal gradient south of the Gomez field located on Figure 3(a) and Figure 3(b) corresponds to a known Ellenburger gas field. This area is characterized by the uplift and folding of pre-Wolfcampian strata overlying basement

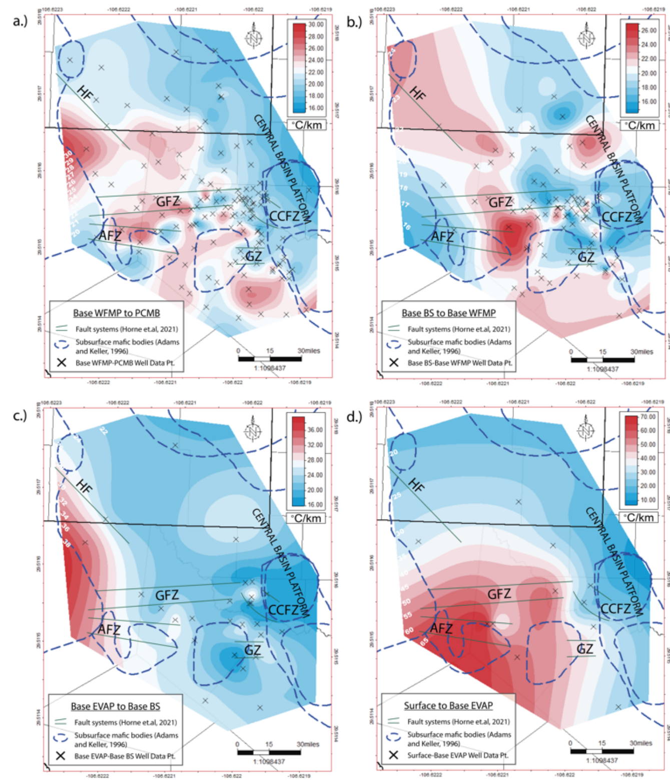

Figure 3: A. Corrected geothermal gradient maps for stratal package 4 from the Base of Wolfcamp to Precambrian basement (Wolfcampian – Precambrian), B. Corrected geothermal gradient maps for stratal package 3 from Base of Bone Spring to base of Wolfcamp (Leonardian – Wolfcampian); C. Corrected geothermal gradient map for stratal package 2 from Base of Salado to base of Bone Spring (Ochoan – Leonardian), D. Stratal package 1: Surface to base of Salado (Present – Ochoan). GFZ = Grisham fault zone, HF = Huapache flexure, AFZ = Apache fault zone, GZ = Gomez field, CCFZ = Coyanosa complex fault zone. Fault zones are modified from Horne et. al. (2021).

highs bounded by high-angle reverse faults. Alternating high and low geothermal gradient values immediately south of the AGM are correlated to patterns of basement faulting along the Grisham fault zone, Huapache flexure, Apache fault zone, and Coyanosa Complex fault zone. These basement-penetrating fault systems promote compartmentalization of geothermal gradient values. This compartmentalization effect is most apparent in stratal package 4 and exhibits a decreasing influence on stratal packages 3, 2, and 1, respectively. The compartmentalization with basement fault blocks supports the presence of intra-basinal hot fluids as a source of heat flow within the basin. Geothermal gradient values south of the AGM are more complex compared to geothermal gradient values north of the AGM and inferred to represent the more variable heat flow related to mafic and sialic intrusive rocks within the basement (Pepper et al., 2020).

Conclusions

Understanding the origin and distribution of radiogenic heat sources is vital to interpreting and predicting trends in geothermal gradient in the Permian Basin. In this study, we have derived a new depth-varying, corrected geothermal gradient and compared these results to various elements which affect heat flow. Our observations indicate that Proterozoic sialic intrusive rocks within the crystalline basement provide a radiogenic heating source for intra-basinal circulation of hot fluids along fault zones. The resulting variable geothermal gradient leads to large spatial variations in gas-to-oil ratios withing drilling target intervals of the Delaware Basin.

Acknowledgments

The authors would like to thank the sponsors at CBTH for their continued financial support.

References

Adams, D.C., and Keller, G.R. ,1996, Precambrian basement geology of the Permian Basin region of west Texas and eastern New Mexico: A geophysical perspective, AAPG Bulletin, v. 80, no. 3, p. 410–431.

Barnes, M.A., Anthony, E.Y., Williams, I., Asquith, G.B., 2002, Architecture of a 1.38–1.34 Ga granite–rhyolite complex as revealed by geochronology and isotopic and elemental geochemistry of subsurface samples from West Texas, USA, Precambrian Research, v. 119, no. 1-4, p. 9-43.

Brown, A., 2019, Post-Permian history of the greater Permian Basin area, in Ruppel, S. C., ed., Anatomy of a Paleozoic basin: the Permian Basin, USA, vol. 1, ch. 5, The University of Texas at Austin, Bureau of Economic Geology Report of Investigations 285; AAPG Memoir 118, p.97–134.

Deighton, I., Tibocha, E., and Dotsey, P., 2014, MaxG and MaxBHT Basin Temperature Modelling Using Bottom Hole Temperature Datasets, Unconventional Resources Technology Conference, Denver, Colorado, August 25-27, 2014.

Ewing, T.E., Barnes, M.A., and Denison, R.E., 2019, Proterozoic foundations of the Permian Basin, West Texas and southeastern New Mexico— a review, in Ruppel, S. C., ed., Anatomy of a Paleozoic basin: the Permian Basin, USA, v. 1, Chapter 3: The University of Texas at Austin, Bureau of Economic Geology Report of Investigations 285; AAPG Memoir 118, p. 43–61.

Fryklund, R., and Stark, P., 2020, Super basins—New paradigm for oil and gas supply, AAPG Bulletin, v. 104, no. 12, p. 2507–2519.

Gardiner, W.B., 1990, Fault fabric and structural subprovinces of the Central Basin Platform: A model for strike-slip movement, in Flis, J.E. and Price, R.C., eds., Permian Basin Oil and Gas Fields: Innovative Ideas in Exploration and Development, Midland, Texas, West Texas Geological Society Publication 90-87, p. 15-27.

Hoak, T., Sunderberg, K., and Ortoleva, P., 1998, Overview of the structural geology and tectonics of the Central Basin Platform, Delaware Basin, and Midland Basin, West Texas and New Mexico, USDOE Technical Report.

Horne, E., Hennings, P., and Zahm, C., 2021, Basement-rooted faults of the Delaware Basin and Central Basin Platform, Permian Basin, West Texas and southeastern New Mexico, in Callahan, O.A., and Eichhubl, P., The Geologic Basement of Texas: A Volume in Honor of Peter T. Flawn: The University of Texas at Austin, Bureau of Economic Geology Report of Investigations No. 286.

Manos, T.A., Perez, N.D., 2018, Thermal Maturity Modeling of Organic-Rich Mudrocks in the Delaware Basin using Raman Spectroscopy of Carbonaceous Material, AAPG ACE Annual Meeting - Salt Lake City, UT. May 23, 2018.

Mosher, S., 1998, Tectonic evolution of the southern Laurentian Grenville orogenic belt, Geological Society of America Bulletin, v. 110, no. 11, p. 1357–1375.

Pepper, A., Doebbert, A., Laigle, J.M., and Laigle, L., 2020, Greater Permian Basin petroleum systems – What are we learning in the transition from conventional to unconventional?, Houston Geological Society Bulletin, v. 62, n.7, p. 13.

Sternbach, C.A., 2020, Super basin thinking: Methods to explore and revitalize the world's greatest petroleum basins, AAPG Bulletin, v. 104, no. 12, p. 2463–2506.

Whaley, J., 2019, Petroleum geology: What is a super basin?, GEO ExPro, v. 16, no. 5, p. 60–64.